

Optical pumping and negative luminescence polarization in charged GaAs quantum dots

Andrew Shabaev,^{*} Eric A. Stinaff,[†] Allan S. Bracker, Daniel Gammon, and Alexander L. Efros[‡]
Naval Research Laboratory, Washington, DC 20375, USA

Vladimir L. Korenev and Igor Merkulov

A. F. Ioffe Physical Technical Institute, St. Petersburg 194021, Russia

(Received 26 August 2008; revised manuscript received 10 November 2008; published 22 January 2009)

Optical pumping of electron spins and negative photoluminescence polarization are observed when interface quantum dots in a GaAs quantum well are excited nonresonantly by circularly polarized light. Both observations can be explained by the formation of long-lived dark excitons through hole spin relaxation in the GaAs quantum well prior to exciton capture. In this model, optical pumping of resident electron spins is caused by capture of dark excitons and recombination in charged quantum dots. Negative polarization results from accumulation of dark excitons in the quantum well and is enhanced by optical pumping. The dark exciton model describes the experimental results very well, including intensity and bias dependence of the photoluminescence polarization and the Hanle effect.

DOI: [10.1103/PhysRevB.79.035322](https://doi.org/10.1103/PhysRevB.79.035322)

PACS number(s): 78.67.Hc, 72.25.Fe, 71.35.Pq

I. INTRODUCTION

Absorption of circularly polarized light by a semiconductor generally leads to optical orientation of electron, hole, and nuclear spins.^{1,2} Photogenerated electron-hole pairs transfer their spin polarization to resident carriers or nuclei, which retain the polarization long after the photogenerated carriers have disappeared. In analogy with atomic physics,^{3,4} the term “optical pumping” refers to the creation of persistent nonequilibrium spin populations. If optical pumping can be done with high efficiency, it provides a way to initialize spins in semiconductor quantum dots (QDs) for quantum information processing.

The polarization of photoluminescence (PL) provides a measure of electron and hole spin polarizations at the moment of recombination. PL polarization is typically positive, meaning it has the same sign as the polarization of the excitation light. However, negative PL polarization is often observed for negatively charged QDs excited by nonresonant light,^{5–13} and reduced polarization was observed for charged GaAs quantum wells (QWs).¹⁴ Negatively charged excitons, such as QD trions or donor-bound excitons, consist of two spin-paired electrons and an unpaired hole. Their PL polarization is determined by the polarization of the unpaired hole spin at the moment of recombination so when their PL polarization is negative, it means that the hole has flipped its spin prior to recombination. Often, a correlation between negative polarization and optical pumping of resident electron spins has been observed.

Several mechanisms have been proposed to explain negative PL polarization. The earliest mechanism is based on the accumulation of “dark” excitons, which do not recombine radiatively, in the two-dimensional (2D) continuum above the QD potential. This was first observed for an ensemble of InP QDs.⁵ We studied the effect in individual charge-tunable GaAs QDs,⁶ observing details that were not available from the earlier ensemble measurements. This allowed us to extend the dark exciton model of Ref. 5, connecting dark exciton accumulation with optical pumping of electron spins. Cortez *et al.*⁷ proposed that negative PL polarization in InAs

QDs under nonresonant excitation is related to electron-hole exchange interactions in the electron spin triplet states of the trion. A similar mechanism was used to explain negative PL polarization observed through resonant excitation of these triplet states.¹⁵ Other mechanisms have been proposed to explain the effect for QDs containing more than one resident electron.^{8,9}

In this paper we describe the dark exciton model and the physical requirements for its applicability. An important element is that exciton capture occurs only if the spin of the QD electron is antiparallel to the electron spin in the exciton. The model is expressed by a nonlinear system of kinetic equations, and the solution provides insight into the origin of both optical pumping and negative PL polarization. The results reproduce the experimental trends, including the dependence of PL polarization on intensity, voltage, and transverse magnetic field (Hanle effect). In our analysis, we look at the connection between negative PL polarization and optical pumping of resident electron spins, which was observed already in the work on InP QDs.⁵ Negative PL polarization is sometimes assumed to be a clear signature of optical pumping, however, we will discuss situations where each exists without the other.

The paper is organized as follows. Section II describes the experimental measurements of PL polarization as a function of applied bias and pumping intensity. The theoretical description of the dark exciton model is presented in Sec. III. We describe simplifying theoretical assumptions and a qualitative explanation of the experimental data, followed by modeling of the bias and intensity dependence of the PL polarization. Section IV reviews the experimental evidence for optical pumping and discusses the mechanism of optical pumping and its implications. In Sec. V, we consider the present model in relation to the triplet model proposed for explanation of negative PL polarization in InAs QDs.

II. EXPERIMENT

The QDs used in this work are created by monolayer fluctuations at the interfaces of a GaAs/Al_{0.3}Ga_{0.7}As quantum

well with a nominal width of 2.8 nm. To allow for the control of charge in the QDs, the quantum well was embedded in a Schottky diode heterostructure grown on an n -type GaAs buffer layer. The layer sequence consists of an n -doped GaAs buffer layer ($\sim 1 \times 10^{18}/\text{cm}^3$), 20 nm doped AlGaAs, 80 nm undoped AlGaAs, 3 nm GaAs QW, 100 nm AlGaAs, and 10 nm GaAs cap. A semitransparent (5 nm) Schottky contact was evaporated on the surface, and an aluminum shadow mask (100 nm) with aperture diameters between 500 nm and 25 μm was fabricated on the sample surface for single QD spectroscopy. The samples were mounted on a nonmagnetic ceramic package and cooled to 8 K in a cold-finger helium flow cryostat. The cryostat head was inserted in the gap of an iron core electromagnet, and luminescence was collected with a microscope objective.

The sample was excited through individual apertures with circularly polarized light from a tunable Ti-Sapphire laser. The laser energy was set to 30 meV above the QD neutral exciton (X^0) PL on the absorption peak for the QW heavy-hole exciton. The laser spot size on the sample was $40 \pm 20 \mu\text{m}$. The PL spectrum was resolved in a 1.5 m triple spectrometer and detected with a multichannel charge coupled device (CCD) or a single-channel avalanche photodiode (APD) combined with a photon counter. In multichannel measurements, a variable liquid crystal retarder (VLCR) controlled the laser polarization. The PL intensity components I^+ (and I^-) of σ^+ (and σ^-) circularly polarized light were analyzed with a VLCR acting as a $\lambda/4$ wave plate followed by a linear polarizer. The PL circular polarization ρ was calculated from $\rho = (I^+ - I^-)/(I^+ + I^-)$. For Hanle effect measurements using the APD, the laser polarization was varied at 42 kHz by a photoelastic quartz modulator in order to suppress dynamic nuclear polarization.

Figure 1(a) shows the PL intensity of a single QD as a function of PL energy and applied bias. Three dominant peaks appear in the spectrum for GaAs QDs, corresponding to the positive trion X^+ (two holes and an electron), the neutral exciton X^0 (electron-hole pair), and the negative trion X^- (two electrons and a hole).¹⁶ Similar charging sequences have been widely discussed for InAs QDs.^{17,18} The assignment of the features for GaAs interface QDs has been established from the Coulomb energy shifts, exchange fine structure, polarization, and charging sequence.^{19,20} Figure 1(b) shows the PL polarization as a function of bias for the peaks in the single QD spectrum of Fig. 1(a). The low degree of circular polarization of the neutral exciton is a well-known consequence of the anisotropic exchange interaction.²¹ Over the same bias range, the PL of the positive trion is positively polarized. The negative trion shows the most interesting behavior, with -20% polarization near the threshold bias (4.1 V), changing to positive polarization as the bias is increased. As the laser intensity is increased, the X^- polarization becomes negative for all values of applied bias (Fig. 2). The power dependence of trion polarization is shown in the lower curve of Fig. 3(b).

As we have noted, the PL polarizations of the trions X^- and X^+ directly reflect the spin of the unpaired minority carrier (hole or electron, respectively) at the moment of recombination. Nonresonant photoexcitation tends to produce polarized electron spins and depolarized hole spins^{22,23} in the

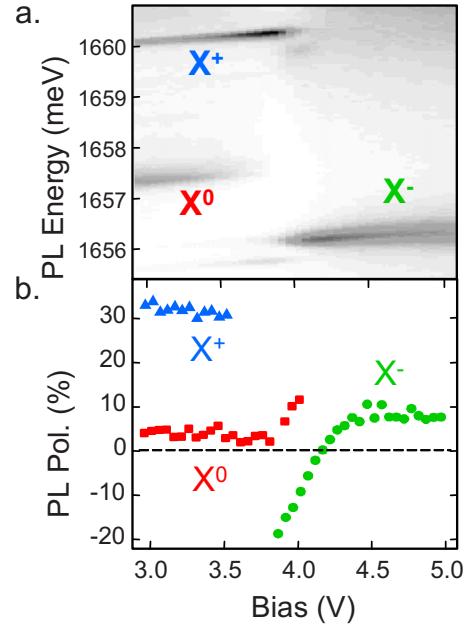


FIG. 1. (Color online) (a) PL intensity of an individual QD (grayscale) for neutral exciton (X^0), negative trion (X^-), and positive trion (X^+) as a function of emitted photon energy and applied bias (Ref. 16). The sample was excited by light with energy 1.686 eV. (b) Photoluminescence polarization measured for the excitons shown in (a).

continuum, so one might initially expect the PL of the trions that form subsequently in QDs to be positively polarized for X^+ (electron polarization) and unpolarized for X^- (hole polarization). The X^+ behavior is consistent with this simple view, but X^- shows both strong positive and negative polarization values depending on the conditions of the experiment. The rest of the paper addresses the reasons for this unusual behavior.

III. DARK EXCITON KINETIC MODEL

A. General description

We propose a straightforward model to account for negative PL polarization of X^- and its dependence on laser inten-

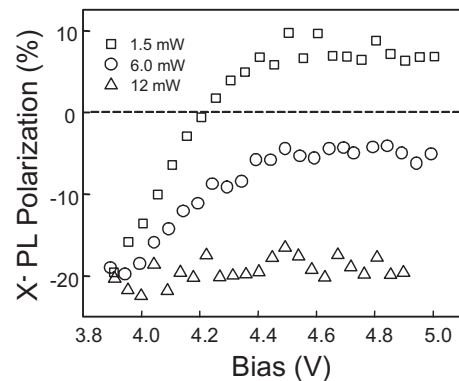


FIG. 2. Photoluminescence polarization of the negative trion (X^-) vs applied bias for three values of the incident laser power.

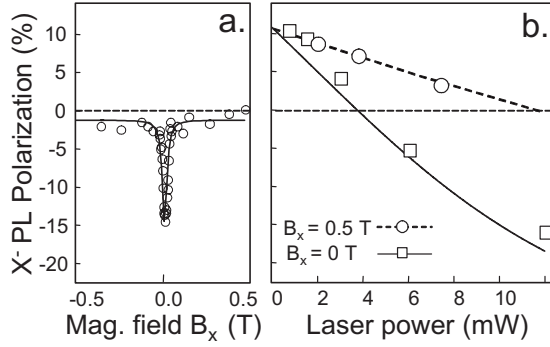


FIG. 3. (a) The Hanle effect measured for the negative trion X^- with 3.9 V applied bias. The peak width is 35 mT corresponding to an electron spin lifetime of 16 ns. (b) Dependence of PL polarization on the laser power $B_x=0$ and 0.5 T with an applied bias of 4.5 V. Symbols are the experimental data. Solid and dashed lines are the results of kinetic modeling using parameters $\tau_b=100$ ps, $W\tau_b=0.25$, $\tau_b/\tau_T=0.2$, $\tau_b/\tau_H=0.05$, $\tau_b/\tau_S=0.03$, and $G_d^\downarrow/G_b^\uparrow=0.08$.

sity and applied bias. Negative PL polarization means that the spin of the photoexcited hole has reversed the sign of its orientation by the time it recombines in a trion X^- . It is not unusual for nonresonant excitation that the photoexcited hole spins are completely depolarized during their thermalization through the strong spin-orbit interactions in the valence band. What was unexpected, however, was that they somehow become repolarized in the opposite direction during the processes of trion formation and relaxation. We propose that this repolarization arises through the predominant capture of dark excitons into charged QDs when trions are formed.

The model is shown schematically in Fig. 4. We consider an ensemble of QDs with concentration N , where each QD contains a single resident electron. The sample is illuminated with circularly polarized light at an energy that excites electron-hole pairs in a two-dimensional continuum, such as the quantum well states of GaAs/AlGaAs natural QDs or the wetting layer of Stranski-Krastanov self-assembled QDs. According to optical selection rules, σ^+ circularly polarized light creates spin-up heavy holes $\uparrow\uparrow$ with $m=+3/2$ spin projection and spin-down electrons \downarrow with $m=1/2$ spin projection along the light propagation direction. This leads to formation of bright excitons with angular momentum projection $m=+1$ ($\uparrow\downarrow$). Excitation with σ^- light would create the opposite spin states. We assume negligible absorption into light hole states and negligible light-heavy mixing.

We assume that before excitons thermalize to the band edge of the continuum, the holes are largely depolarized, while the electrons remain highly polarized.²² Efficient spin relaxation of holes in excitons is well known and results from spin-orbit coupling in valence-band continuum states. As a result, σ^+ -polarized excitation produces a mixture of bright excitons ($\uparrow\downarrow$ with $m=+1$) and dark excitons ($\downarrow\downarrow$ with $m=-2$), whose direct optical recombination is forbidden according to the selection rules. These thermalized excitons are produced at the band edge with generation rates G_b^\uparrow and G_d^\downarrow , where $G_b^\uparrow \geq G_d^\downarrow$, and the rates are equal if hole depolarization is complete. After thermalization, hole spin flips are inhibited, and interconversion of bright and dark excitons is much less important. Bright excitons can recombine radiatively

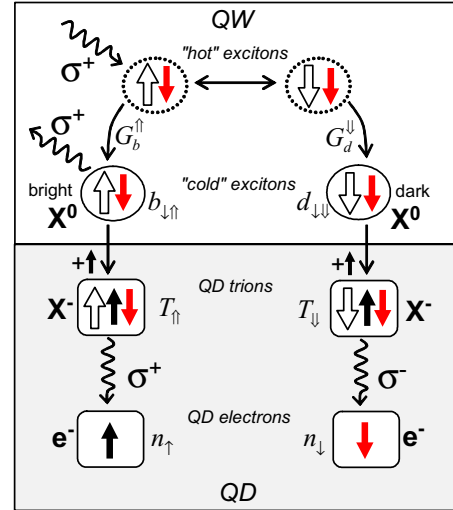


FIG. 4. (Color online) Pictorial summary of relaxation processes that influence polarization of negative trions, as considered in the kinetic model. Upper panel: Bright excitons are excited in the quantum well continuum, and hole polarization is lost. A mixture of bright and dark “cold” excitons is created at the QW band edge. At the band edge, bright excitons can decay radiatively or be captured in the QDs, but dark excitons can only be captured. Lower panel: excitons are captured by the QDs with resident electron spin antiparallel to the exciton electron spin. The trions created from bright excitons emits σ^+ polarized light, while trions created from dark excitons are σ^- polarized. The dark exciton pathway optically pumps the QD resident electron spin because it replaces the original resident electron (spin up) with the photoelectron (spin down).

(rate $1/\tau_b$) but dark excitons cannot. Excitons can also form trions in charged QDs, and for dark excitons, trion formation is the only disappearance mechanism to first approximation. The concentrations of all possible exciton spin states at the band edge are described by $b_{\uparrow\downarrow}$ and $b_{\downarrow\uparrow}$ for bright excitons and $d_{\uparrow\downarrow}$ and $d_{\downarrow\uparrow}$ for dark excitons. We neglect $b_{\downarrow\uparrow}$ and $d_{\uparrow\uparrow}$ because σ^+ -polarized light creates only \downarrow electrons, and electron spin relaxation is slow.

Trions form when neutral excitons are captured into charged QDs. The ground-state trions are singlet states $X_{+3/2}^- \equiv \uparrow\downarrow\uparrow$ and $X_{-3/2}^- \equiv \downarrow\downarrow\uparrow$, consisting of a singlet electron pair and an unpaired hole. The trion concentrations are T_{\uparrow} and T_{\downarrow} . The trions decay radiatively with rate $1/\tau_T$, emitting σ^+ and σ^- photons, respectively. The corresponding PL intensities I^+ and I^- are proportional to the trion spin populations, and the degree of PL polarization that we measure in our experiment is $\rho_{X^-} = (T_{\uparrow} - T_{\downarrow}) / (T_{\uparrow} + T_{\downarrow})$.

The formation and decay of excitons and trions are shown schematically in Fig. 4 for the case of σ^+ -polarized excitation. The kinetic equations describing these dynamics can be written in the following form:

$$\frac{db_{\downarrow\uparrow}}{dt} = G_b^\uparrow - \frac{b_{\downarrow\uparrow}}{\tau_b} - Wn_{\uparrow} \times b_{\downarrow\uparrow} - \frac{b_{\downarrow\uparrow} - d_{\downarrow\downarrow}}{\tau_H}, \quad (1a)$$

$$\frac{dd_{\downarrow\downarrow}}{dt} = G_d^\downarrow - Wn_{\uparrow} \times d_{\downarrow\downarrow} - \frac{d_{\downarrow\downarrow} - b_{\downarrow\uparrow}}{\tau_H}, \quad (1b)$$

$$\frac{dT_{\uparrow}}{dt} = Wn_{\uparrow} \times b_{\downarrow\uparrow} - \frac{T_{\uparrow}}{\tau_T}, \quad (1c)$$

$$\frac{dT_{\downarrow}}{dt} = Wn_{\downarrow} \times d_{\downarrow\downarrow} - \frac{T_{\downarrow}}{\tau_T}, \quad (1d)$$

$$\frac{dn_{\uparrow}}{dt} = -\Omega S_x - Wn_{\uparrow}(b_{\downarrow\uparrow} + d_{\downarrow\downarrow}) + \frac{T_{\uparrow}}{\tau_T} - \frac{n_{\uparrow} - n_{\downarrow}}{\tau_S}, \quad (1e)$$

$$\frac{dn_{\downarrow}}{dt} = \Omega S_x + \frac{T_{\downarrow}}{\tau_T} - \frac{n_{\downarrow} - n_{\uparrow}}{\tau_S}, \quad (1f)$$

$$\frac{dS_x}{dt} = \frac{\Omega}{2}(n_{\uparrow} - n_{\downarrow}) - \frac{S_x}{\tau_S} - \frac{W}{2}S_x(b_{\downarrow\uparrow} + d_{\downarrow\downarrow}), \quad (1g)$$

$$N = n_{\uparrow} + n_{\downarrow} + T_{\uparrow} + T_{\downarrow}. \quad (1h)$$

These equations include rate expressions for concentrations of all spin states of bright and dark excitons [Eqs. (1a) and (1b)], trions [Eqs. (1c) and (1d)], and electrons [Eqs. (1e)–(1g)]. The symbols n_{\uparrow} and n_{\downarrow} are the concentrations of QDs with resident electron spins up (\uparrow) and down (\downarrow), respectively. We also assume (for now) that each QD has an electron and the total concentration of QDs is N , which leads to the constraint of Eq. (1h). The symbols τ_S and τ_H represent the electron and hole spin relaxation times, respectively. Equations (1e)–(1g) are written using a quasi-two-dimensional approximation for electron spin relaxation time, although for QDs this time will include nuclear contributions due to electron localization. We have neglected the anisotropic exchange interaction between bright excitons $\uparrow\downarrow$ and $\downarrow\uparrow$ because this process is suppressed for the nearly free excitons prior their capture in QDs.²⁴ The system of Eq. (1) is not symmetric with respect to $b_{\uparrow\downarrow}$ and $b_{\downarrow\uparrow}$ or $d_{\uparrow\uparrow}$ and $d_{\downarrow\downarrow}$ because of the σ^+ polarized excitation and the long electron spin memory.

The rate of exciton capture by charged QDs (i.e., trion formation) depends generally on the spin configuration of the QD electron and the exciton electron. The triplet configuration (parallel electron spins) is less strongly bound than the singlet configuration (antiparallel spins). In a shallow QD, as in GaAs quantum wells,²⁵ the triplet levels may be unbound. Deep GaAs defects also show preferential electron capture for spin singlet states.^{26,27} Here, we assume strict selectivity—capture occurs only for the electron singlet configuration. With this assumption, the rates of exciton capture into a QD with spin up \uparrow and spin down \downarrow are proportional to $Wn_{\uparrow}(b_{\downarrow\uparrow} + d_{\downarrow\downarrow})$ and $Wn_{\downarrow}(b_{\uparrow\downarrow} + d_{\uparrow\uparrow})$, respectively, where W is the spin-independent bimolecular capture cross section of the QD. Because of these exciton capture terms, the system of Eq. (1) is nonlinear, leading to nonlinear optical pumping of electron spins. Note that the second term is not included in Eq. (1) because we have assumed that $b_{\downarrow\uparrow}$ and $d_{\uparrow\uparrow}$ are zero.

The system of Eq. (1) also accounts for electron spin precession in the x - z plane caused by a transverse magnetic field \mathbf{B} along the y direction. The precession occurs with the frequency $\Omega = g_e \mu_B B$, where g_e is the electron g factor and μ_B is

the Bohr magneton. We include this term in order to describe the Hanle effect. For the same reason, Eq. (1g) is required to describe the evolution of the electron spin polarization S_x along the x axis.

In the results that follow, we note that the model describes an ensemble of QDs, not an isolated dot. Although the measurements probe an individual QD directly, the states of other QDs and the continuum are important to the observed single QD properties. This is a natural situation when the laser energy is tuned above the QD potential because an exciton captured into one dot will have previously interacted with electrons and excitons over a wider region. Moreover, an individual dot may not be a typical example of the ensemble. In this work, we have measured dots that are on the low-energy side of the ensemble spectrum; so under some conditions, they may be charged while most of the ensemble is neutral. In this situation, a charged dot that we measure behaves as a probe of an uncharged ensemble.

B. Qualitative analysis

Although the system of Eq. (1) is nonlinear and can generally only be solved numerically, the assumption of strong spin selectivity for exciton capture leads to a very simple expression for the degree of trion PL polarization ρ_{X^-} . Making the steady-state approximation [left side of Eqs. (1a)–(1f) set to zero], one easily obtains an expression for ρ_{X^-} in terms of the concentration of bright and dark excitons at the band edge:

$$\rho_{X^-} \equiv \frac{T_{\uparrow} - T_{\downarrow}}{T_{\uparrow} + T_{\downarrow}} = \frac{b_{\downarrow\uparrow} - d_{\downarrow\downarrow}}{b_{\downarrow\uparrow} + d_{\downarrow\downarrow}}. \quad (2)$$

This expression shows that negative polarization of trions excited by σ^+ polarized light is observed only if the dark exciton concentration exceeds the bright exciton concentration. Within the same approximation, one can write for the bright and dark exciton populations:

$$b_{\downarrow\uparrow} = \frac{G_b^{\uparrow}(Wn_{\uparrow} + 1/\tau_H) + G_d^{\downarrow}/\tau_H}{Wn_{\uparrow}(Wn_{\uparrow} + 2/\tau_H) + (Wn_{\uparrow} + 1/\tau_H)/\tau_b},$$

$$d_{\downarrow\downarrow} = \frac{G_d^{\downarrow} + b_{\downarrow\uparrow}/\tau_H}{Wn_{\downarrow} + 1/\tau_H}. \quad (3)$$

These expressions are further simplified in the limit of very long hole spin relaxation times ($\tau_H = \infty$). With this simplification, the exciton concentrations become

$$b_{\downarrow\uparrow} = \frac{G_b^{\uparrow}}{Wn_{\uparrow} + 1/\tau_b}, \quad (4a)$$

$$d_{\downarrow\downarrow} = \frac{G_d^{\downarrow}}{Wn_{\downarrow}}. \quad (4b)$$

Equation (4) gives an intuitive understanding of the conditions that lead to negative PL polarization. The concentration of bright excitons is determined by both radiative decay ($1/\tau_b$) and exciton capture by the charged QD, i.e., trion

formation (Wn_{\uparrow}), while the concentration of dark excitons is determined only by the latter. This situation can lead to dark exciton accumulation and negative polarization ($d_{\downarrow\downarrow} > b_{\downarrow\uparrow}$). This is most likely to occur when holes are initially depolarized ($G_d^{\downarrow} = G_b^{\uparrow}$), but it can even happen when dark exciton generation is inefficient ($G_d^{\downarrow} < G_b^{\uparrow}$) if $Wn_{\uparrow} \ll 1/\tau_b$. In other words, a small concentration n_{\uparrow} of spin-up resident electrons is able to reverse the sign of hole polarization by prolonging the time it takes for an exciton to form a trion. An exciton diffuses through the 2D layer until it encounters a QD electron \uparrow . During this time, bright excitons disappear through recombination, but dark excitons survive until the antiparallel electron spin becomes available. The resulting accumulation of dark excitons leads to negative PL polarization according to Eq. (2).

One process that reduces n_{\uparrow} is optical pumping, which we consider in more detail in Sec. IV. Here, we analyze this effect only in the limit of low laser intensity. In this case, Eq. (1) gives the following decrease in the concentration n_{\uparrow} of electron spins:

$$n_{\uparrow} = N/2 - G_d^{\downarrow}\tau_s/2, \quad (5)$$

which is controlled by the dark exciton generation rate G_d^{\downarrow} (proportional to laser power). One can see from Eq. (5) that a longer electron spin relaxation time τ_s makes the electron spin optical pumping more efficient. Experimentally, we cannot control the intrinsic spin relaxation time, but we can artificially manipulate it with the Hanle effect, where the spin precesses in a transverse magnetic field, thereby suppressing the optical pumping.

Using Eq. (1), we can also derive the expression for the electron spin polarization, $P_e = (n_{\uparrow} - n_{\downarrow})/N$, in the limit of weak pumping intensity:

$$P_e = -G_d^{\downarrow}\tau_s/N. \quad (6)$$

We note that this polarization depends only on the dark exciton generation rate and not on bright exciton parameters. This clearly emphasizes that optical pumping of electron spins and negative PL polarization, which does depend on bright excitons [Eq. (2)], are two distinct phenomena.

C. Bias and intensity dependence of PL polarization

When the diode containing the QDs is forward biased, QDs and quasicontinuum states are charged with electrons. This charging strongly affects the trion formation kinetics. With many electrons present, the ensemble trion formation rate (proportional to Wn_{\uparrow}) is high so that both bright and dark excitons form trions with equal probability [Eqs. (3) and (4)], and the PL polarization is positive. On the other hand, near the threshold bias where the trion peak first appears in the single QD spectrum (4 V), there are few electrons elsewhere in other QDs. With Wn_{\uparrow} small, excitons wait for a longer time before being captured in a charged QD. Slower trion formation leads to a build-up of dark excitons and to negative PL polarization for QDs that contain an electron.

Using the system of Eq. (1) we can model the experimental data shown in Fig. 2. We plot polarization as a function of the concentration of dots that contain one electron. In order

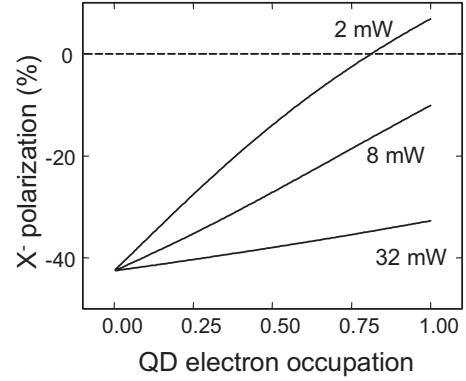


FIG. 5. Negative trion PL polarization degree as a function of average QD electron occupation calculated for three pumping powers. The parameters used in the kinetic model are $\tau_b=100$ ps, $W\tau_b=0.27$, $\tau_b/\tau_T=1$, $\tau_b/\tau_S=0.035$, and $\tau_b/\tau_H=0.05$. The horizontal axis in this figure scales monotonically with the applied bias in Fig. 2 although the quantitative relation between the two is unknown.

to do this, we relax the normalization condition in Eq. (1h), allowing some fraction of the QDs to be uncharged. Although the direct relationship between concentration of charged QDs and diode bias is unknown, the parameters are closely related because forward bias lowers the QD potentials below the Fermi level, charging them with electrons. The modeling results shown in Fig. 5 reproduce the qualitative trends of Fig. 2 very well: the PL polarization increases with the number of QD electrons (applied bias), and it decreases with laser intensity.

The modeling of low electron concentrations in Fig. 5 also highlights the distinction between negative polarization and optical pumping. For all laser intensities, the trion polarization reaches its most negative value when the electron concentration is zero. As we noted above, this effect results simply from the absence of electrons and the accumulation of dark excitons. Optical pumping is not required. Indeed, we showed in Figs. 2(a) and 2(c) of Ref. 6 that some negative PL polarization persists even at high transverse magnetic fields B_x , where electron spins are depolarized by the Hanle effect. Negative polarization of trions mainly reflects the properties of the exciton ensemble, not the electron spins, which are very few in number under these conditions. However, we will see in Sec. IV that those electron spins are strongly pumped by the abundant dark excitons.

At higher values of electron concentration, the effects of optical pumping are seen in the laser intensity dependence. In Figs. 2 and 5, the trion polarization becomes more negative as the laser intensity increases, and the change is greater for higher electron concentrations. The values of the parameters used to generate these curves are listed in the figure caption and correspond to typical values for GaAs interface QDs.

IV. OPTICAL PUMPING

The dark exciton model is strongly confirmed by our experimental study of the PL polarization in a transverse magnetic field (Hanle effect). The Hanle effect provides direct

evidence of optical pumping, as discussed in Ref. 6. We review that experimental evidence here and compare it with the results of the model.

Figure 3(a) shows the Hanle effect for a charged GaAs QD. The peak is inverted,^{5,14} in contrast to the usual Hanle effect for bulk semiconductors.¹ This inverted peak establishes a connection between optical pumping of electron spins and negative (or reduced) PL polarization: When the magnetic field B_x (Voigt geometry) is applied, the electron spins are depolarized, leading to an increase in the PL polarization. Holes have a small in-plane g factor and are insensitive to the applied field. Polarized electron spins therefore make the PL polarization more negative. We will show below that the peak depth is closely related to the degree of electron spin polarization.

The width of the Hanle peak gives additional evidence that resident electron spins are probed. The electron spin lifetime is inversely proportional to the peak width, and we find under typical conditions that the X^- negative polarization is eliminated by only 35 G.⁶ A standard formula¹ for Hanle peak widths gives an electron spin lifetime of 16 ns. This lifetime is much too long to be explained by electrons in excitonic states, which have lifetimes limited by radiative recombination. The X^- singlet state itself should not contribute to the Hanle effect because its electron spins are paired and have no polarization. We therefore conclude that the Hanle effect probes optically pumped resident electron spins.

Equation (6) shows directly that the electron spin polarization is connected with dark exciton generation. The mechanism for optical pumping implied by Eq. (1) and Fig. 4 is very simple: when a dark exciton $\downarrow\downarrow$ is captured into a charged QD, the spin-down hole recombines with the resident electron \uparrow , leaving the *optically created* electron \downarrow in its place. On the other hand, when a bright exciton is captured, that same exciton recombines and the original resident electron remains—there is no net change in the QD electron spin.

The dependence of the PL polarization on laser power is shown in Fig. 6(a) for transverse magnetic fields of 0 (solid lines) and 0.5 T (dashed lines).²⁸ A similar pair of curves is included as a fit of the experimental data in Fig. 3(b). The effect of electron depolarization (the Hanle peak depth) is the difference between the dashed and solid curves. The modeling in Fig. 6 was conducted for two ratios of the dark-to-bright exciton generation rates: $G_d^\downarrow/G_b^\uparrow < 1$. This ratio is related to the hole relaxation rate for hot QW excitons and is larger for excitation with higher photon energies. The simulations demonstrate the decrease in PL polarization caused by optical pumping, including negative polarization at higher laser intensities.

Interestingly, the experimental points in Fig. 3(b) show a modest decrease in the PL polarization even for $B_x=0.5$ T when the resident electron spins are completely depolarized by the transverse magnetic field. In this situation, something other than optical pumping must be responsible for the dark exciton accumulation. A reduced probability for biexciton formation is one possibility that would become more important for higher laser intensities, in agreement with the experimental data. In our model, this situation is already accounted for to the maximum extent because biexciton formation is not considered (effectively forbidden). To reproduce the

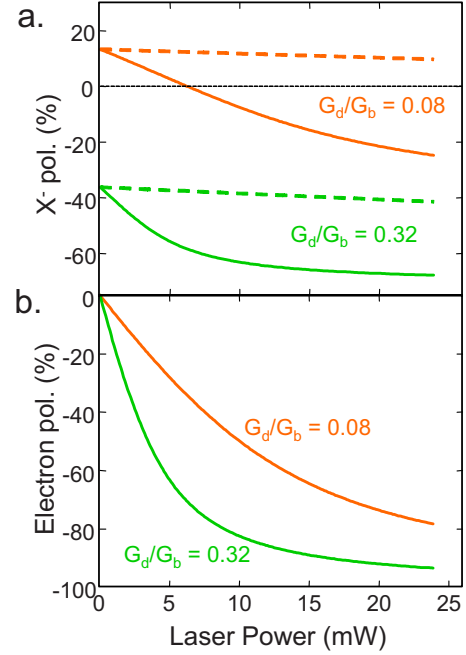


FIG. 6. (Color online) (a) Calculated trion PL polarization vs laser intensity for $B_x=0$ (solid lines) and 0.5 T (dashed lines) for two values of the ratio of generation rates $G_d^\downarrow/G_b^\uparrow$ for dark and bright excitons. The ratio $G_d^\downarrow/G_b^\uparrow$ is changed experimentally by changing the laser excitation energy (see Ref. 6). (b) Electron spin polarization in zero magnetic field vs pumping power. Other parameters were $\tau_b=100$ ps, $W\tau_b=0.27$, $\tau_b/\tau_T=1$, $\tau_b/\tau_S=0.035$, and $\tau_b/\tau_H=0.05$.

measured trion polarization with the simulations, we had to use a long trion radiative lifetime $\tau_T=10\tau_b$. Indeed, the trion radiative lifetime in QDs can be longer than that of excitons,²⁹ however, the fitting parameter τ_T/τ_b is larger than we would expect. We therefore believe it is likely that other processes not included in our model contribute to the $B_x=0.5$ T data, but this does not qualitatively affect our interpretation of the experimental results. In the simulations discussed below, we use the more conventional assumption that $\tau_T=\tau_b$.

The Hanle peak depth is a much better measure of optical pumping than the absolute PL polarization. The PL polarization is related to the relative concentrations of dark and bright excitons [Eq. (2)], but only the generation rate of dark excitons matters for optical pumping [Eq. (6)]. This is because bright exciton capture has no effect on the resident electron spin. Optical pumping may reduce the positive polarization without actually making it negative.¹⁴ In the experimental data of Fig. 3(b), an inverted Hanle peak is observed even when the PL polarization is positive. A more pronounced example of this situation exists when the ratio $G_d^\downarrow/G_b^\uparrow$ is small. This is true when hole spin flips are suppressed by photoexcitation at lower energy (closer to the QW band edge). This causes the PL polarization to be much more positive, as seen in the curves for $G_d^\downarrow/G_b^\uparrow=0.08$ in Fig. 6(a) and in Fig. 2 of Ref. 6. However, despite the positive PL polarization for $B_x=0.5$ T, the Hanle peak depth is large as long as the laser intensity is high enough.

The simulation in Fig. 6 allows us to relate the Hanle peak depth to the actual electron polarization. In addition to the

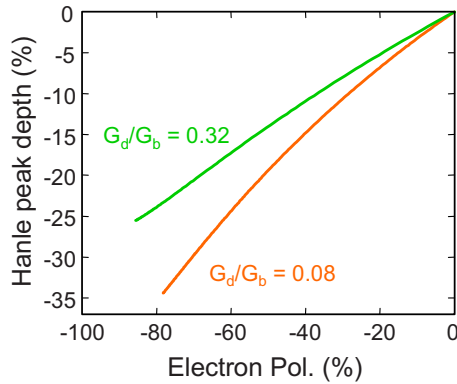


FIG. 7. (Color online) Hanle peak depth vs electron spin polarization obtained parametrically from the calculations shown in Fig. 6. The Hanle peak depth corresponds to the difference between the X^- polarization values for $B_x=0$ and 0.5 T in Fig. 6(a).

trion polarizations, we also calculated the electron polarization as a function of laser intensity, as shown in Fig. 6(b). We then used laser intensity as a parametric variable to connect the y axes of Figs. 6(a) and 6(b). Figure 7 shows the resulting plot of the peak depth [calculated from Fig. 6(a)] vs the electron polarization of Fig. 6(b). We find a nearly linear relationship between these two properties that depends only slightly on the ratio of generation rates. This allows us to roughly quantify the efficiency of optical pumping from our measurements. Based on the typical values of the parameters for GaAs QDs, we estimate from the simulation that electron spin polarization is more than twice as large as the measured peak depth and may reach values as high as 60% in our experiments.

V. DISCUSSION

The dark exciton model for optical pumping and negative PL polarization should be generally applicable to QDs excited through a higher-energy continuum. In the experimental part of this work, we have considered GaAs/AlGaAs QDs, however, the proposed mechanism and theoretical modeling are quite general and should apply to strained self-assembled InAs QDs as well. Nevertheless, the values of key kinetic parameters could limit the importance of the dark exciton mechanism in InAs QDs. For example, exciton capture may be less spin selective in the stronger confinement potential of InAs QDs, allowing triplet trions to form with high probability. This opens up spin relaxation channels that are not considered in this work. Also, the longer bright exciton lifetimes and rapid exciton capture times in InAs dots would limit dark exciton accumulation, as pointed out in Ref. 8. Dark exciton accumulation in the wetting layer may not be as important for InAs QDs because both electrons and holes are strongly bound and can be captured by the QD as independent particles.

A widely discussed model for negative PL polarization in InAs QDs involves excited states of the trion, where one electron resides in a p -like orbital. Electron spin triplet and singlet states exist,^{7,8,15,30,31} and spin-selective relaxation is induced by the electron-hole symmetric and asymmetric ex-

change interactions. Cortez *et al.*⁷ and Laurent *et al.*⁸ discussed the results of simulations based on nonresonant excitation followed by triplet trion formation and relaxation. Those results reproduced the measured time dependence of PL polarization and the dependence on longitudinal magnetic field. The assumptions of the mechanism implied that the electron spins were optically pumped.

The InAs trion triplet states have also been studied resonantly with photoluminescence excitation spectroscopy.¹⁵ One of the two bright triplet components was observed to have very strong negative PL polarization, while the other was positively polarized. These observations were explained with a variation in the model discussed in Refs. 7 and 8. In the analysis in Ref. 15, negative polarization was understood to occur in the absence of optical pumping—the QD contained a spin-down resident electron both before and after exciton capture and trion recombination.

A pronounced difference between our results on GaAs QDs and some results on InAs QDs is in the degree of correlation between negative polarization and optical pumping. We have shown here that the two are only loosely related, but measurements of dynamic nuclear polarization in InAs QDs suggest that they can be very closely linked.^{32,33} There, the sign of the trion PL polarization was found to match the sign of the nuclear polarization and, by implication, the sign of the QD electron spin. Surprisingly, the nuclear polarization sometimes had the opposite sign from the photoelectron polarization. In contrast, our measurements in GaAs QDs (Ref. 6) showed that the nuclei were always polarized in the same sense as the photoelectron spin (and the QD spin) but not necessarily the same as the trion. If the trion, nuclear, and QD electron spin polarizations are all tightly correlated in InAs QDs, then optical pumping may occur by a substantially different mechanism than that described in this work. Lai *et al.*³³ proposed that the interaction of the QD electron spin with electron spins in the nearby doped GaAs layer plays an important role.

Very high pumping efficiency has been achieved through resonant excitation of individual quantum dots containing a resident electron^{34,35} or hole.³⁶ This optical pumping technique is similar in concept to the original technique discovered for atoms by Kastler and co-workers.^{3,4} One electron spin state is excited to the trion, and if recombination produces the opposite electron spin state with even a small probability, it will be trapped there, and the QD becomes transparent to further photoexcitation. If relaxation of the electron spin is much slower than trion recombination to the pumped spin state, very high pumping efficiency (>99%) can be achieved. This approach is highly energy specific and therefore addresses a single QD. With nonresonant excitation, an entire ensemble can be pumped, however, the system does not become transparent, and with multiple relaxation pathways, high pumping efficiency is much harder to achieve.

VI. CONCLUSION

The model presented here describes negative photoluminescence polarization and optical pumping of electron spins in quantum dots. It reproduces the experimental observations

of PL polarization as a function of laser intensity and applied bias. An inverted Hanle curve gives a clear experimental signature of optical pumping. Although the PL polarization may be reduced to negative values by optical pumping, the model and the data show that negative polarization is not a definitive signature of optical pumping. Both phenomena result from dark exciton accumulation in quasicontinuum states, followed by spin-dependent capture in QDs and finally radiative recombination. The model suggests that the

degree of electron spin polarization in the experiments may be as high as 60%.

ACKNOWLEDGMENTS

This research was supported by ONR, NSA/ARO, RFBF, and NSF under Grant No. PHY99-07949. A.L.E. would like to express appreciation for the hospitality of the Kavli Institute for Theoretical Physics.

*Present address: Department of Computational and Data Sciences, George Mason University, Fairfax, VA 22030.

†Present address: Department of Physics & Astronomy, Ohio University, Athens, OH 45701.

‡efros@dave.nrl.navy.mil

¹*Optical Orientation*, edited by F. Meier and B. P. Zakharchenya (Elsevier, Amsterdam, 1984).

²A. S. Bracker, D. Gammon, and V. L. Korenev, *Semicond. Sci. Technol.* **23**, 114004 (2008); D. Gammon, Al. L. Efros, J. G. Tischler, A. S. Bracker, V. L. Korenev, and I. A. Merkulov, in *Quantum Coherence, Correlation, and Decoherence in Semiconductor Nanostructures*, edited by T. Takagahara (Academic, San Diego, 2003).

³A. Kastler, *J. Phys. Radium* **11**, 255 (1950).

⁴J. Brossel, A. Kastler, and J. Winter, *J. Phys. Radium* **13**, 668 (1952).

⁵R. I. Dzhioev, B. P. Zakharchenya, V. L. Korenev, P. E. Pak, D. A. Vinokurov, O. V. Kovalenkov, and I. S. Tarasov, *Phys. Solid State* **40**, 1587 (1998).

⁶A. S. Bracker, E. A. Stinaff, D. Gammon, M. E. Ware, J. G. Tischler, A. Shabaev, Al. L. Efros, D. Park, D. Gershoni, V. L. Korenev, and I. A. Merkulov, *Phys. Rev. Lett.* **94**, 047402 (2005).

⁷S. Cortez, O. Krebs, S. Laurent, M. Sénès, X. Marie, P. Voisin, R. Ferreira, G. Bastard, J. M. Gérard, and T. Amand, *Phys. Rev. Lett.* **89**, 207401 (2002).

⁸S. Laurent, M. Sénès, O. Krebs, V. K. Kalevich, B. Urbaszek, X. Marie, T. Amand, and P. Voisin, *Phys. Rev. B* **73**, 235302 (2006).

⁹V. K. Kalevich, I. A. Merkulov, A. Y. Shiryayev, K. V. Kavokin, M. Ikezawa, T. Okuno, P. N. Brunkov, A. E. Zhukov, V. M. Ustinov, and Y. Masumoto, *Phys. Rev. B* **72**, 045325 (2005).

¹⁰V. K. Kalevich, M. Ikezawa, T. Okuno, A. Y. Shiryayev, A. E. Zhukov, V. M. Ustinov, P. N. Brunkov, and Y. Masumoto, *Phys. Status Solidi B* **238**, 250 (2003).

¹¹R. Oulton, A. Greilich, S. Y. Verbin, R. V. Cherbunin, T. Auer, D. R. Yakovlev, M. Bayer, I. A. Merkulov, V. Stavarache, D. Reuter, and A. D. Wieck, *Phys. Rev. Lett.* **98**, 107401 (2007).

¹²M. Ikezawa, B. Pal, Y. Masumoto, I. V. Ignatiev, S. Y. Verbin, and I. Y. Gerlovin, *Phys. Rev. B* **72**, 153302 (2005).

¹³J. Berezovsky, M. H. Mikkelsen, O. Gywat, N. G. Stoltz, L. A. Coldren, and D. D. Awschalom, *Science* **314**, 1916 (2006).

¹⁴R. I. Dzhioev, V. L. Korenev, B. P. Zakharchenya, D. Gammon, A. S. Bracker, J. G. Tischler, and D. S. Katzer, *Phys. Rev. B* **66**, 153409 (2002).

¹⁵M. E. Ware, E. A. Stinaff, D. Gammon, M. F. Doty, A. S.

Bracker, D. Gershoni, V. L. Korenev, Ș. C. Bădescu, Y. Lyanda-Geller, and T. L. Reinecke, *Phys. Rev. Lett.* **95**, 177403 (2005).

¹⁶The electron charging transition in Fig. 1(a) occurs at an applied bias of 3.8 V due to a non-Ohmic back contact to the diode. For an Ohmic contact, the transition would occur below 1 V.

¹⁷R. J. Warburton, C. Schäfflein, D. Haft, F. Bickel, A. Lorke, K. Karrai, J. M. Garcia, W. Schoenfeld, and P. M. Petroff, *Nature (London)* **405**, 926 (2000).

¹⁸M. Ediger, P. A. Dalgarno, J. M. Smith, B. D. Gerardot, R. J. Warburton, K. Karrai, and P. M. Petroff, *Appl. Phys. Lett.* **86**, 211909 (2005).

¹⁹J. G. Tischler, A. S. Bracker, D. Gammon, and D. Park, *Phys. Rev. B* **66**, 081310(R) (2002).

²⁰A. S. Bracker, E. A. Stinaff, D. Gammon, M. E. Ware, J. G. Tischler, D. Park, D. Gershoni, A. V. Filinov, M. Bonitz, F. M. Peeters, and C. Riva, *Phys. Rev. B* **72**, 035332 (2005).

²¹D. Gammon, E. S. Snow, B. V. Shanabrook, D. S. Katzer, and D. Park, *Phys. Rev. Lett.* **76**, 3005 (1996).

²²T. C. Damen, L. Viña, J. E. Cunningham, J. Shah, and L. J. Sham, *Phys. Rev. Lett.* **67**, 3432 (1991).

²³M. Paillard, X. Marie, P. Renucci, T. Amand, A. Jbeli, and J. M. Gérard, *Phys. Rev. Lett.* **86**, 1634 (2001).

²⁴M. Dyakonov, X. Marie, T. Amand, P. LeJeune, D. Robart, M. Brousseau, and J. Barrau, *Phys. Rev. B* **56**, 10412 (1997).

²⁵A. J. Shields, M. Pepper, M. Y. Simmons, and D. A. Ritchie, *Phys. Rev. B* **52**, 7841 (1995).

²⁶C. Weisbuch and G. Lampel, *Solid State Commun.* **14**, 141 (1974).

²⁷D. Paget, *Phys. Rev. B* **30**, 931 (1984).

²⁸Laser power is included in the calculation through the expression $G_b^{\uparrow} = (1-R)\alpha L_z \frac{P}{n\hbar\omega A_{\text{spot}}}$, where P is the laser power, $R=0.3$ is the reflection coefficient, $\alpha=2 \times 10^4 \text{ cm}^{-1}$ is the absorption coefficient, $n=0.5 \times 10^{10} \text{ cm}^{-2}$ is the QD density, $\hbar\omega=1.6 \text{ eV}$ is the photon energy, $L_z=3 \times 10^{-7} \text{ cm}$ is the quantum well width, and $A_{\text{spot}}=\pi(40 \mu\text{m})^2/4$ is the cross-sectional area of the laser beam.

²⁹The suppression of the radiative decay time of the trion compared to the exciton is connected with influence of the interparticle Coulomb interactions on the electron and hole wave functions.

³⁰K. V. Kavokin, *Phys. Status Solidi A* **195**, 592 (2003).

³¹I. A. Akimov, A. Hundt, T. Flissikowski, and F. Henneberger, *Appl. Phys. Lett.* **81**, 4730 (2002).

³²B. Eble, O. Krebs, A. Lemaître, K. Kowalik, A. Kudelski, P. Voisin, B. Urbaszek, X. Marie, and T. Amand, *Phys. Rev. B* **74**, 081306(R) (2006).

- ³³C. W. Lai, P. Maletinsky, A. Badolato, and A. Imamoğlu, Phys. Rev. Lett. **96**, 167403 (2006).
- ³⁴M. Atatüre, J. Dreiser, A. Badolato, A. Högele, K. Karrai, and A. Imamoğlu, Science **312**, 551 (2006).
- ³⁵X. D. Xu, Y. W. Wu, B. Sun, Q. Huang, J. Cheng, D. G. Steel, A. S. Bracker, D. Gammon, C. Emary, and L. J. Sham, Phys. Rev. Lett. **99**, 097401 (2007).
- ³⁶B. D. Gerardot, D. Brunner, P. A. Dalgarno, P. Ohberg, S. Seidl, M. Kroner, K. Karrai, N. G. Stoltz, P. M. Petroff, and R. J. Warburton, Nature (London) **451**, 441 (2008).